Fabrication and Characterization of Low-Loss Optical Fibers Containing Rare-Earth Ions

SIMON B. POOLE, DAVID N. PAYNE, ROBERT J. MEARS, MARTIN E. FERMANN, AND RICHARD I. LAMING

Abstract—**Low-loss fibers containing rare-earths have been produced with high absorption levels in the visible and near infrared regions. Although containing relatively large quantities of rare-earth impurity dopants, the fibers possess low-loss windows where the attenuation is similar to that observed in undoped fibers. This attribute makes the fibers attractive for use in long distributed sensors, as well as low-threshold fiber lasers. Fiber characteristics relevant to these two applications are uniformity of dopant incorporation, absorption and fluorescence spectra, and fluorescence lifetime. These measurements are presented, together with their respective temperature dependences. The fiber fabrication method is described and results given for Nd^{3+}-, Er^{3+}-, and Tb^{3+}-doped fibers.**

I. Introduction

As LIGHTWAVE technology matures and conventional fibers become commonplace, attention is being increasingly directed to the fabrication of special fibers dedicated to particular functions. For example, the fiber guiding structure can be readily modified to provide polarization-holding properties, or a given dispersion characteristic. In addition to variations in waveguide structure, however, it is evident that modifying the materials from which the fibers are constructed can yield large improvements in the performance of optical fiber sensors (for a review see ref. [1]), or of transmission components such as isolators [2]. In this respect, glasses containing rare-earth ions are of particular interest, since their use is well known in both active (laser) and passive bulk-optical devices.

The introduction of Tb^{3+} or Ho^{3+} ions into a glass matrix is known to increase the Verdet constant of the glass [3], thus potentially improving the sensitivity of the fiber in magnetometers [4] and current measuring devices [5]. Similarly, it is thought that the nonlinear optical properties of a fiber may be increased by the incorporation of Yb^{3+} [6].

Short lengths of heavily-doped neodymium glass have already been employed as single-point temperature sensors, exploiting either the change in absorption spectrum [7] or the fluorescence decay time [8]. The extension of these techniques to distributed temperature sensing over long lengths of fiber requires much smaller rare-earth concentrations, as well as very low intrinsic fiber losses.

Multimode fibers containing relatively large concentrations of neodymium also have been reported, fabricated from either compound glasses [9] or silica [10]. Lasers employing short lengths of these fibers have shown multimode stimulated emission at or near a wavelength of 1.06 μm. Similarly, erbium glass lasers [11] which operate at a wavelength within the popular third window for optical communications (~ 1.55 μm), also are known and would make a particularly attractive fiber device.

With the recent emphasis on single-mode transmission and fiber devices, it is worthwhile reexamining this early laser work with a view to constructing single-mode fiber lasers and amplifiers in configurations that require much longer lengths of active fiber, for example, ring-resonator lasers and long, distributed wideband amplifiers. At their operating wavelength, such devices demand the very low losses inherent in telecommunications grade fiber, as well as the close proximity of large impurity absorption bands for the purpose of pumping to an excited state. This requirement and the need to end-pump long single-mode active fiber devices has led us to explore the fabrication of low-loss fibers containing much lower concentrations of rare-earths than previously considered.

In this paper we describe a technique for fabricating silica based multi- and single-mode fibers doped with low levels (<0.25 wt/o) of rare-earth ions. The dopant incorporation can be achieved without significantly compromising the inherently low losses of the fiber. As examples, the characteristics of fibers containing Nd^{3+}, Er^{3+}, and Tb^{3+} are presented and their suitability for fiber sensors assessed. The use of these fibers in various laser configurations is described in an accompanying paper [12].

II. Fabrication

To ensure low losses in rare-earth doped fibers, it is advantageous to exploit existing vapor-phase techniques (e.g., the MCVD process) and high-purity precursor materials. The rare-earth halides are ideal starting materials, as they are readily available in high (>99.99 percent) purity. However, since they are hygroscopic and have high melting points ($>500°C$), a number of modifications must

Manuscript received November 25, 1985. This work was supported in part by the U.K. Science and Engineering Research Council (RJM, MEF, RIL), by a Readership (DNP) and Research Fellowship (SBP) provided by Pirelli General PLC, and by the JOERS project.

The authors are with the Optical Fiber Group, Department of Electronics and Information Engineering, Southampton University, Southampton, England.

IEEE Log Number 8608481.

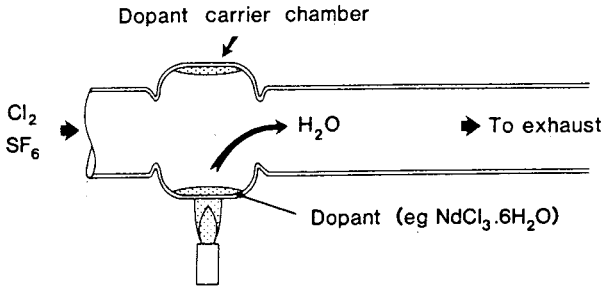

Fig. 1. Substrate tube incorporating dopant carrier chamber, showing drying technique for rare-earth chlorides.

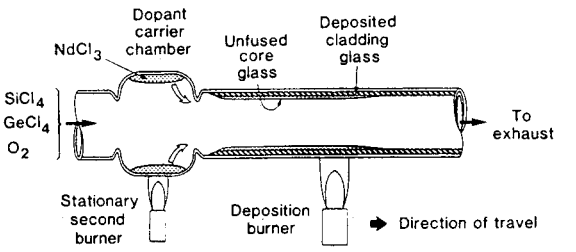

Fig. 2. Core-deposition stage for production of fibers doped with rare-earths.

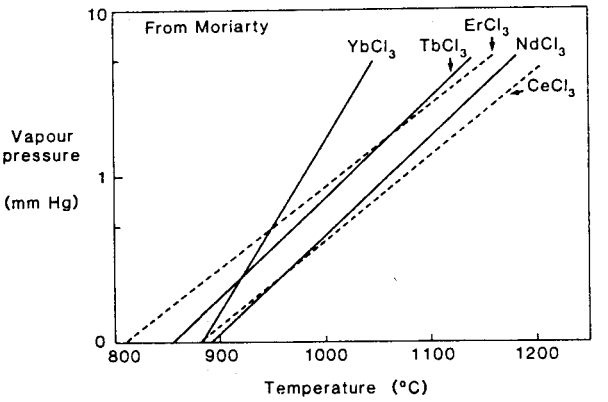

Fig. 3. Dependence of vapor pressure on temperature for typical rare-earth chlorides.

be made to the MCVD process in order to incorporate the dopants without affecting the fiber loss. It should be noted that the technique we have developed is not limited to the rare-earth elements, but may be applied to the incorporation of any dopant from a precursor material which is a solid at or near room temperature, for example, the transition metals.

Fabrication can be considered in four stages:

A. Preconditioning and Drying of Rare-Earth Chloride

A standard MCVD substrate tube (O.D. 25 mm, 1.5-mm wall) is modified by the addition of a dopant carrier chamber upstream from the deposition tube, as shown in Fig. 1. The deposition tube is mounted in a preform lathe and the required solid dopant precursor material, e.g., $NdCl_3.6H_2O$ (99.9 percent pure, melting point = 758°C), is introduced into the carrier chamber. The carrier chamber is then gently heated by a temperature-controlled burner to about 100°C above the melting point of the dopant while flowing a drying gas, either Cl_2 or SF_6, at a rate of 1 l/min. The dopant melts and, on cooling, forms a fused, anhydrous layer on the inside of the carrier chamber.

This refining stage is designed to both fully dehydrate the dopant crystals and to prevent free particulates from passing down the tube during subsequent deposition stages. However, fibers fabricated using only this single drying stage showed unacceptably high OH^--absorption losses due to residual water of crystallization in the fused dopant. Consequently, a second drying stage was introduced during the core deposition, as will be described later.

B. Cladding Deposition

Initially, any rare-earth material carried downstream during the refining stage is removed from the walls of the deposition tube by gas-phase etching using SF_6 [13] (1600°C, 0.8 l/min). A conventional MCVD cladding glass is then deposited to give a cladding/core diameter ratio of greater than 7:1. Typically a SiO_2-P_2O_5-F-matched clad is used, but preforms also have been fabricated using SiO_2-B_2O_3 and undoped SiO_2.

C. Core Deposition

Here a number of further modifications to the standard MCVD technique are made to ensure rare-earth incorporation and reduce OH^- contamination. These will be described with reference to Fig. 2.

The dopant carrier chamber is preheated to a controlled temperature above 1000°C by a stationary burner to increase the vapor pressure of the fused rare-earth chloride. The required temperature is determined by the vapor-pressure characteristics of the material and the required dopant level in the finished fiber. Vapor pressure curves for some typical rare-earth chlorides are given in Fig.3 [14]. It can be seen that a temperature of around 1000°C is sufficient to give a vapor pressure of about 1 Torr. If necessary, an increase in the vapor pressure could be obtained by using the appropriate iodide or bromide salts.

During core deposition, the reactants (typically $GeCl_4$ and $SiCl_4$) are mixed with oxygen and passed through the heated dopant chamber, where controlled amounts of rare-earth halide are entrained in the gas flow. Since the chamber temperature is insufficient to oxidize the reactants, they are oxidized as normal in the downstream hot zone to produce deposited core layers containing low levels of rare-earths. However, the temperature of the MCVD hot zone is chosen such that it is not high enough to fuse the deposited core glass layers. This enables further drying of the materials to be performed.

Analysis of the dopant concentration in the fiber core shows higher dopant levels with increasing carrier chamber temperature, as predicted by the vapor pressure curves. A wide range of dopant concentration levels can thus be obtained by careful control of the temperature.

D. Core Drying and Fusion

After deposition, the porous core layer is further dried by heating to 900°C for 30 min with a traversing burner,

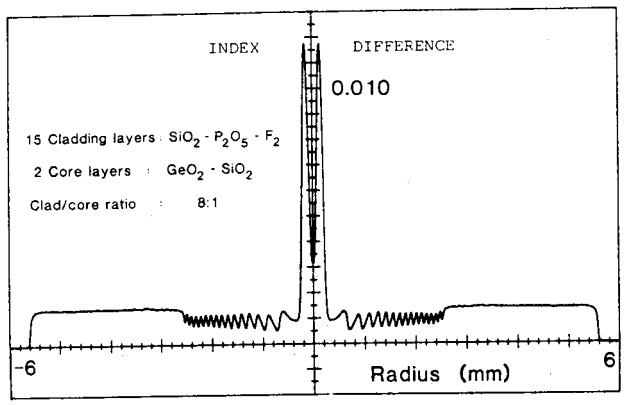

Fig. 4. Refractive-index profile of rare-earth doped preform. Deposited cladding is SiO_2-P_2O_5-F. Core is GeO_2-SiO_2 containing ~450 ppm Tb^{3+}.

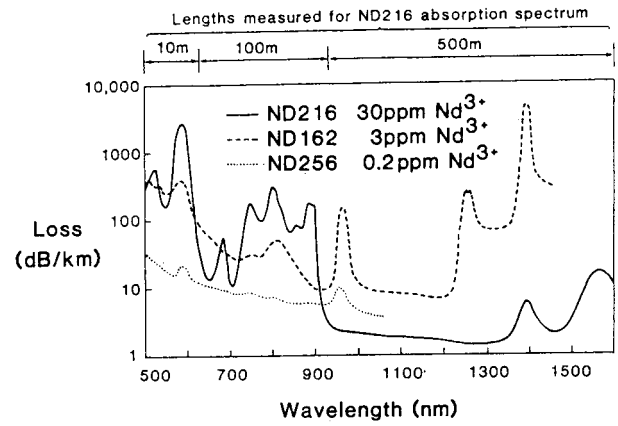

Fig. 5. Absorption spectra of fibers containing various concentrations of Nd^{3+} ions (as marked), showing windows of very low loss. For comparison, fiber attenuation without second drying stage (ND 162) exhibits large OH^- absorption band at 1390 nm. The lengths marked at the top of the diagram indicate the fiber lengths used to obtain the absorption spectrum of ND216.

while flowing chlorine gas through the tube (1 l/min). The technique is similar to that used for the dehydration of VAD preforms [15]. The unsintered layer is then fused to form a glassy layer, with the addition of helium, if required, to prevent bubble formation [16]. Preform collapse and fiber drawing are conventional.

E. Fabrication Results

A wide range of single and multimode fibers containing rare-earths have been fabricated including highly birefringent "Bow-tie" fibers [13]. Core index differences of between 0.2 and 1.2 percent and dopant incorporation levels between 0.2 and 900 ppm have been achieved. These results indicate the versatility of the technique and its applicability to many types of fiber design.

The level of rare-earth incorporation is insufficient to significantly affect the core refractive index [10]. Consequently, the refractive-index profile is due solely to the conventional MCVD dopants and can be varied accordingly. The profile of a Tb^{3+}-doped preform is shown in Fig. 4 and is virtually identical to that obtained without rare-earth doping.

The fabrication technique also can be applied to core compositions other than the GeO_2-SiO_2 glass used here, for instance the P_2O_5-SiO_2 [17] and Al_2O_3-SiO_2 [18] glass systems. Moreover, the technique may be used to introduce impurity dopants into the deposited cladding glass.

III. Characteristics of Fibers Containing Rare-Earth Ions

Dopants which have been successfully incorporated into fibers include Nd^{3+}, Er^{3+}, Tb^{3+}, and Eu^{3+} ions. In the results presented below, the dopant concentrations were confirmed by comparing the measured absorption spectra of the drawn fibers with previously published data for rare-earth ions in high-silica bulk glasses [19]. The results that follow are biased toward Nd^{3+}-doped fibers, since this material is better characterized in the literature.

A. Absorption Spectra

Measurement of the absorption spectra of rare-earth doped fibers poses a number of problems owing to the difficulty of measuring losses which vary by several orders of magnitude across the spectrum. A multiple cutback technique in combination with attenuation equipment optimized for dynamic range was used to overcome these difficulties. A white-light source and a scanning double monochromator provided the fiber input, while the output power was measured using either a Si or, for longer wavelengths, a liquid N_2 cooled Ge photodiode. The double monochromator reduced the stray light in the system and allowed an attenuation in excess of 48 dB to be measured in single-mode fibers with a 2-nm spectral resolution (c.f. 35 dB in most instruments).

Various fiber lengths were measured, depending upon the regions of the spectrum under test and the results rescaled and combined to give absorption spectra with extremely high dynamic ranges. For example, the absorption spectrum of the Nd^{3+}-doped fiber number ND216 illustrated in Fig. 5 was determined using lengths of 10, 100, and 500 m, as indicated on the graph, and shows a measurement range of 3000 dB/km.

A possible source of error in the measurement is the presence of excited state fluorescence, a proportion of which is received by the detector. The effect reduces the apparent loss within the absorption bands. However, it can be calculated that the fluorescence has a negligible effect on measurement accuracy and this was confirmed by using blocking filters.

The absorption spectra for three fibers containing different levels of Nd^{3+} dopant are shown in Fig. 5. Strong characteristic Nd^{3+} absorptions in the visible and near infrared regions can be clearly seen, together with a low-loss window (<2 dB/km for fiber ND216) between 950 and 1350 nm. Significantly, this includes the Nd^{3+} laser wavelength around 1.60 μm, where the loss is only 1.8 dB/km. These loss levels are not dissimilar to those observed in telecommunications-grade fibers. The small loss penalty is believed to be due to increased scatter in the glass as a result of the presence of large impurity ions, rather than to absorption band tails.

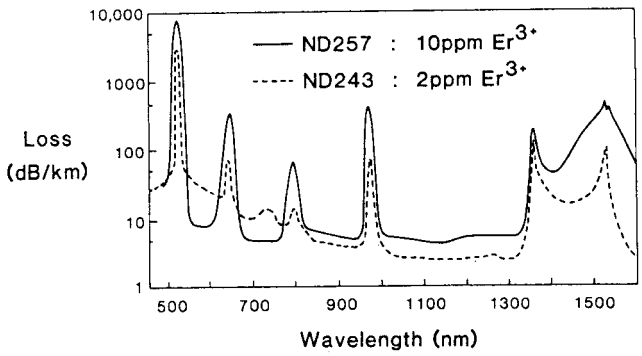

Fig. 6. Absorption spectra of fibers containing 2 and 10-ppm Er^{3+} ions.

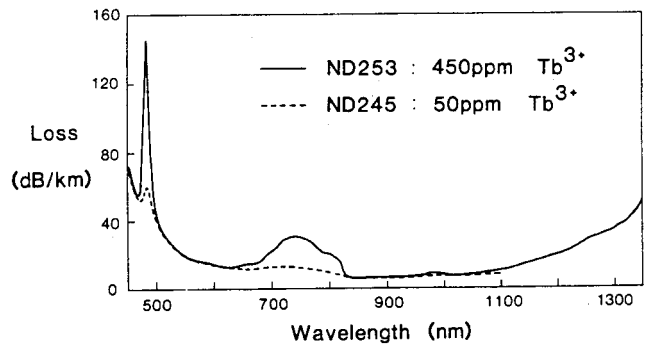

Fig. 7. Absorption spectra of fibers containing 50- and 450-ppm Tb^{3+} ions.

The efficiency of the techniques used to dry both the precursor and deposited materials is demonstrated by comparing the OH^--absorption bands at 1390 nm for fibers ND162 and ND216 (Fig. 5.) No attempt was made to dry either the precursor or deposited materials for fiber ND162, resulting in an OH^--impurity level of ~65 ppm. For fiber ND216, however, the two-stage drying technique results in a considerably reduced OH^--absorption peak of only 5 dB/km at 1390 nm, which corresponds to an OH^--impurity level of ~80 ppb.

The absorption spectra for two fibers containing different levels of Er^{3+} ions are shown in Fig. 6. Strong Er^{3+}-absorption bands can be clearly seen at 520, 980, and 1536 nm with, again, regions of low loss close to the absorption peaks. This is particularly marked in fiber ND257 where, despite the extremely high loss (~9000 dB/km) in the absorption band at 520 nm, the loss falls to a remarkable 25 dB/km at 540 nm, a mere 20 nm away.

The absorption spectra for two fibers containing Tb^{3+} ions are shown in Fig. 7. Although containing relatively high dopant concentrations, the fibers show only a few, low-intensity peaks compared to the Nd^{3+}-and Er^{3+}-doped fibers described previously. The effect is typical of Tb^{3+} ions in glass and is due to the low absorption cross section of the Tb^{3+} ion within the wavelength range of measurement. Note that the loss increase beyond 1 μm for both fibers are bend edges, as the fibers were designed for use at wavelengths below 600 nm, where the Tb^{3+} ion is known to fluoresce (see below).

The temperature dependence of the absorption spectra (Fig. 8) is important for both fiber sensors and lasers. The

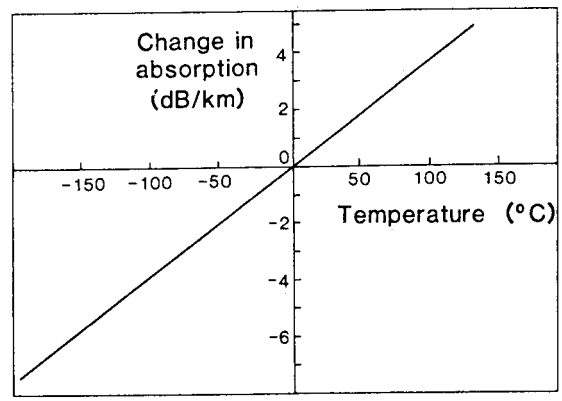

Fig. 8. Temperature variations of absorption at 600 nm in a fiber doped with ~0.2-ppm Nd^{3+}.

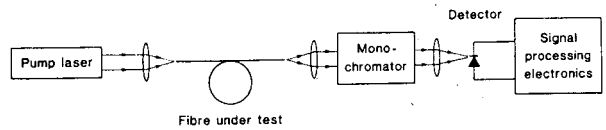

Fig. 9. Schematic of equipment for measurement of fluorescence characteristics. Signal-processing equipment consists of a phase-sensitive detector for fluorescence spectra or a computer-controlled digital averager for fluorescence lifetime measurements.

TABLE I
SPECIFICATIONS OF PUMP LASERS USED IN MEASUREMENTS OF FIBER FLUORESCENCE CHARACTERISTICS

Dopant	Pump Laser Type	Pump Wavelength (nm)	Pump Output Power (mW)
Nd^{3+}	Semiconductor	780	1
Er^{3+}	Argon-ion	514	200
Tb^{3+}	Argon-ion	488	50

fiber used was multimode (40-μm core, 125-μm cladding) and contained 0.2-ppm Nd^{3+}. The absorption spectrum at 25°C was given in Fig. 5 (fiber ND256.) Over the range from −196°C (liquid nitrogen) to +125°C, the fiber loss at 600 nm (i.e., the tail of the 590-nm absorption band) shows a linear dependence with temperature, which is promising for use as a temperature sensor.

B. Fluorescence Spectra

The fluorescence spectra of the fibers was measured using the equipment shown schematically in Fig. 9. The laser used as the pump source depends upon the fiber under investigation, since for efficient excitation it is necessary to match the pump wavelength to an impurity absorption band. The wavelengths and output powers of the lasers used for each rare-earth are shown in Table I. The detector was either a Si or a liquid N_2 cooled Ge photodiode, depending on the wavelength of interest. The signal was processed with a phase-sensitive detector.

Referring to Fig. 10, the Nd^{3+} fiber shows fluorescence bands centered on wavelengths of 940, 1088, and 1370

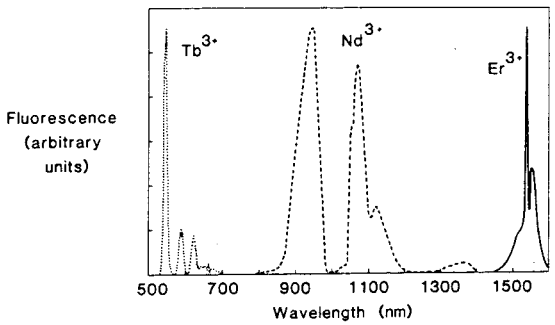

Fig. 10. Fluorescence spectra of Nd^{3+}-, Er^{3+}-, and Tb^{3+}-doped fibers.

nm, corresponding to emissions from the $^4I_{3/2}$ state to the $^4I_{13/2}$, $^4I_{11/2}$, and $^4I_{9/2}$ levels. Note that the fluorescence peaks are shifted to slightly longer wavelengths than normal in glass as a result of the silica host [10], [20]. The broad fluorescence band centered at 1.088 μm has enabled the development of a neodymium fiber laser with an extremely wide tuning range of 80 μm [12].

As expected in a three-level system, the fluorescence of the Er^{3+}-doped fiber coincides with an absorption band at the fluorescence wavelength. The fluorescence measured corresponds to a transition from the $^4I_{13/2}$level to the $^4I_{15/2}$ ground level and again, the extensive width of this band has led to the development of a broadly tunable CW laser, in this case tunable between 1.529 and 1.553 μm [12].

The fluorescence spectrum of the Tb^{3+}-doped fiber contains visible fluorescence bands at 545, 590, and 625 nm. These correspond to transitions from the $^5D_4$ level to the $^7F_5$, $^7F_4$ and $^7F_3$ levels, respectively. A further weak fluorescence band centered around 670 nm also can be seen and is believed to be a combination of the fluorescence due to $^5D_4$ to $^7F_2$, $^7F_1$ and $^7F_0$ transitions.

C. Fluorescence Lifetimes

A knowledge of the fluorescence decay time is required to permit calculations of fiber laser saturation intensities and lasing thresholds. In addition, the temperature dependence of the fluorescence lifetime is of interest for sensor applications. The fluorescence decay characteristics were investigated with the equipment shown schematically in Fig. 9, with a laser again chosen to match the absorption bands of the fiber under test. The signal-processing electronics now consist of a computer-controlled digital averager triggered by the laser pump.

The fluorescence lifetime of the Nd^{3+}-doped fibers was measured using a frequency-doubled Q-switched Nd-YAG laser (wavelength 532 nm, pulse width 90 ns) as the pump source. A 1/e fluorescence decay time of 470 μs at both 940 and 1088 nm was measured, which is in good agreement with previously published results [20]. For the Er^{3+}-doped fibers, a 1/e decay time of 14 ms was obtained using a mechanically-chopped argon-ion laser beam operating at 514 nm as the pump. This is again in good agreement with previously results [11].

A more detailed analysis of the fluorescence decay was made for the Nd^{3+}-doped fibers. A curve fitting routine was used to obtain the instantaneous 1/e decay time and Fig. 11 shows this value plotted against time after the excitation pulse. It may be seen that the instantaneous value of the fluorescence lifetime increases with time, a phenomenon which has been previously noted [21] and which is due to the statistical distribution of the Nd^{3+} ion in the glass matrix.

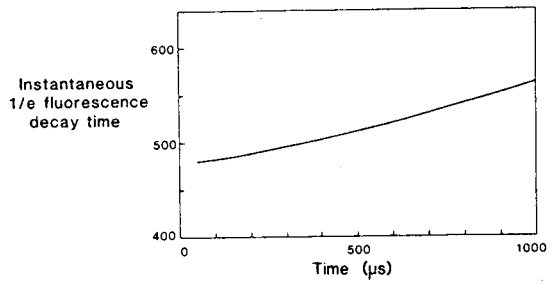

Fig. 11. Variation in instantaneous 1/e fluorescence decay time for a Nd^{3+}-doped fiber plotted against time-after-excitation.

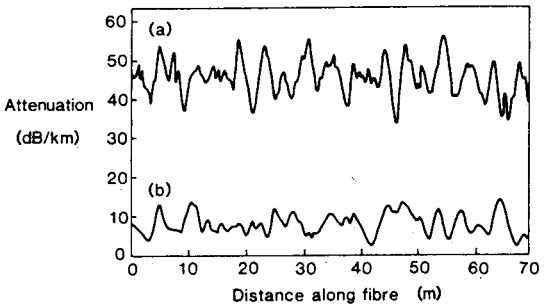

Fig. 12. Local attenuation of fibers measured using an OTDR technique, showing average uniformity over length. (a) Nd^{3+}-doped fiber. (b) Undoped reference fiber.

Initial measurements of the temperature dependence of the fluorescence decay in Nd^{3+}-doped fibers show a decrease of approximately 2 percent in the 1/e fluorescence lifetime over the temperature range 0 to 100°C. This is accompanied by a 10-percent decrease in the fluorescence output level due to a reduction in the quantum efficiency of the fluorescence process [22].

D. Consistency of Dopant Incorporation with Length

The use of rare-earth doped fibers as distributed sensors [1] or fiber lasers [12] requires a uniform dopant incorporation along the fiber length. The wavelength-tunable backscatter technique [23] was used to obtain length resolution of the dopant absorption bands and the result obtained at 620 nm for a Nd^{3+}-doped single-mode fiber is shown in Fig. 12, together with a reference result for an undoped fiber.

No variation in the average absorption level, and hence amount of dopant incorporated, is visible along the 80-m length of the doped fiber, thus confirming the high degree of control in the fabricated process. The noise levels visible on both traces are due to well-known measurement limitations [24] and are not associated with rapid dopant fluctuations.

IV. Discussion

The application of the rare-earth doped fibers described here has already been demonstrated. Lasing action has been reported at a wavelength of 1.088 μm in Nd^{3+}-doped fibers [25] and at 1.536 μm in Er^{3+}-doped fibers [12]. The very low thresholds reported are due in part to the extremely low losses of the fibers, which further emphasizes the importance of the techniuqes developed to remove OH^--impurity ions.

The possibility of using rare-earth doped fiber as the sensing element in a distributed temperature sensor has been mentioned earlier. Calculations for a distributed sensor based on the temperature variation of the Nd^{3+}-absorption bands indicate that an accuracy of 3°C with a resolution of 5 m could be easily obtained over a 200-m length of fiber, using a backscatter technique similar to that described in [26]. Further improvements may be obtained by the use of a dopant with a greater change in absorption with temperature.

V. Conclusions

A simple, reproducible fiber fabrication technique has been developed which allows the incorporation of uniformly low levels of rare-earth ions as impurity dopants in the core of many types of optical fibers. The technique is not limited to the rare-earth elements, but could be applied to any dopant with a solid precursor material, for instance the transition metals.

Fibers have been fabricated containing various rare earths with dopant levels of between 0.2 and 990 ppm (0.25 wt/o). Remarkably, all exhibit windows in which losses are comparable with conventional fibers, despite the close proximity of very high-loss dopant absorption bands. The low fiber losses combined with the consistency of dopant incorporation along the fiber length make the fibers suitable for use in distributed sensor applications.

It is clear that rare earth-doped fibers of the type described here will find many applications in laser and nonlinear devices, signal processing, and switching. An early indicator of the potential is the ease with which low-threshold single-mode fiber lasers can be constructed using either Nd^{3+}-or Er^{3+}-doped fibers.

Acknowledgments

The authors would like to thank Dr. M. P. Gold for help with the backscatter measurements and L. Reekie for useful discussions and assistance with the fluorescence measurements.

References

[1] D. N. Payne, "Fibers for sensors," in *Proc. 2nd Int. Conf. Opt. Fiber Sensors* (Stuttgart, W. Germany), 1984, pp. 353-360.
[2] K. Shiraishi, "Fiber-embedded micro-Faraday rotator for the infrared," *Appl. Opt.*, vol. 24, pp. 951-954, Apr. 1985.
[3] N. F. Borelli, "Faraday rotation in glasses," *J. Chem. Phys.*, vol. 41, pp. 3289-3293, Dec. 1964.
[4] G. W. Day, D. N. Payne, A. J. Barlow, and J. J. Ramskov-Hansen, "Faraday rotation in coiled, monomode optical fibers: Isolators, filters, and magnetic sensors," *Opt. Lett.*, vol. 7, pp. 238-240, Dec. 1982.
[5] A. M. Smith, "Polarization and magnetooptical properties of optical fibers," *Appl. Opt.*, vol. 17, pp. 52-56, 1978.
[6] M. Watanabe, H. Yokota, and M. Hoshikawa, "Fabrication of Yb_2O_3-SiO_2 core fiber by a new process," in *Proc. 11th Eur. Conf. Opt. Commun.* (Venice, Italy), 1985, pp. 15-18.
[7] E. Snitzer, W. W. Morey, and W. H. Glenn, "Fiber-optic rare-earth temperature sensors," in *Proc. 1st Int. Conf. Opt. Fiber Sensors*, (London, England), 1983, pp. 79-81.
[8] K. T. V. Gratten and A. W. Palmer, "A simple, inexpensive neodymium rod fiber-optic temperature sensor," in *Proc. 3rd Int. Conf. Opt. Fiber Sensors*, (San Diego, CA), 1984, p. 142.
[9] E. Snitzer, "Neodymium glass laser," in *Proc. 3rd Int. Conf. Solid-State Lasers*, (Paris, France), 1963, pp. 999-1019.
[10] J. Stone and C. A. Burrus, "Neodymium-doped silica lasers in end-pumped fiber geometry," *Appl. Phys. Lett.*, vol. 23, pp. 388-389, Oct. 1973.
[11] E. Snitzer and R. Woodcock, "Yb^{3+}-Er^{3+} glass laser," *Appl. Phys. Lett.*, vol. 6, pp. 45-46, Feb. 1965.
[12] L. Reekie, R. J. Mears, S. B. Poole, and D. N. Payne, "Tunable single-mode fiber lasers," This issue, pp. 956-960.
[13] R. D. Birch, D. N. Payne, and M. P. Varnham, "Fabrication of polarization-maintaining fibers using gas-phase etching," *Electron. Lett.*, vol. 18, pp. 1036-1038, Nov. 1982.
[14] J. L. Moriarty, "Vapor pressures of yttrium and rare-earth chlorides above their melting points," *J. Chem. Eng. Data*, vol. 8, pp. 422-424, June 1963.
[15] S. Sudo, M. Kawachi, T. Edahiro, T. Izawa, T. Shioda, and H. Gotoh, "Low-OH-content optical fiber fabricated by vapor-phase-axial-deposition method," *Electron. Lett.*, vol. 14, pp. 534-535, Aug. 1978.
[16] K. L. Walker, J. W. Harvey, F. T. Geyling, and S. R. Nagel, "Consolidation of particulate layers in the fabrication of optical-fiber preforms," *J. Amer. Ceram. Soc.*, vol. 63, pp. 96-102, 1980.
[17] D. N. Payne and W. A. Gambling, "New silica-based low-loss optical fiber," *Electron. Lett.*, vol. 10, pp. 289-290, July 1974.
[18] J. R. Simpson and J. B. MacChesney, "Optical fibers with an Al_2O_3-doped silicate core composition," *Electron. Lett.*, vol. 19, pp. 261-262, 1983.
[19] H. L. Smith and A. J. Cohen, "Absorption spectra of cations in alkali-silicate glasses of high ultra-violet transmission," *Phys. Chem. Glasses*, vol. 4, pp. 173-187, Oct. 1963.
[20] H. Namikawa, K. Arai, K. Kumata, Y. Ishii, and H. Tanaka, "Preparation of Nd-doped SiO_2 glass by plasma torch CVD," *Jap. J. Appl. Phys.*, vol. 21, pp. L360-L362, June 1982.
[21] D. C. Brown, *High-peak-power Nd: Glass laser systems*. New York: Springer-Verlag, 1981, ch. 1, p. 5.
[22] B. Hok and L. Jonsson, "Pressure sensor with fluorescence decay as information carrier," in *Proc. 2nd Int. Conf. Opt. Fiber Sensors* (Stuttgart, W. Germany), 1984, pp. 391-394.
[23] A. J. Conduit, A. H. Hartog, and D. N. Payne, "Spectral- and length-dependent losses in optical fibers investigated by a two-channel backscatter technique," *Electron. Lett.*, vol. 16, pp. 77-78, Jan. 1980.
[24] M. P. Gold and A. H. Hartog, "Determination of structural parameter variations in single-mode optical fibers by time-domain reflectometry," *Electron. Lett.*, vol. 18, pp. 489-490, June 1982.
[25] R. J. Mears, L. Reekie, S. B. Poole, and D. N. Payne, "Neodymium-doped silica single-mode fiber lasers," *Electron. Lett.*, vol. 21, pp. 738-740, Aug. 1985.
[26] A. H. Hartog, "A distributed temperature sensor based on liquid-core optical fibers," *J. Lightwave Technol.*, vol. LT-1, pp. 498-509, Sept. 1983.

*

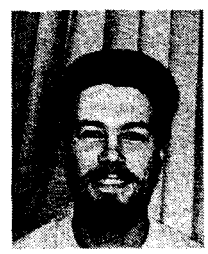

Simon B. Poole was born in Watford, England, in 1958. He received the B.Sc. in electrical and electronic engineering from the University of Nottingham in 1979.

In 1981, he joined the Optical Fiber Group at Southampton University as a research student working on optical-fiber fabrication and characterization. He is now the Pirelli Research Fellow within the Group. His current research interests include novel dopant materials and their uses in fiber devices.

David N. Payne was born in Lewes, England, on August 13, 1944, and educated in Central Africa. He received the B.Sc. in electrical engineering, the Diploma in quantum electronics, and the Ph.D degree from the University of Southampton, England.

In 1972, he was appointed the Pirelli Research Fellow in the Department of Electronics, University of Southampton and in 1977 became Senior Research Fellow. He is currently Research Reader and directs the Optical Fiber Group, consisting of some 40 members. Since 1969 his research interests have been in Optical Communications and have included preform and fiber fabrication techniques, optical propagation in multimode and single-mode fibers, fiber and preform characterization, wavelength-dispersive properties of optical-fiber materials, optical-transmission measurements, and fiber devices. He has published over a 100 papers and holds 11 patents. Currently his main fields of interest are special fibers, fiber lasers and devices, fiber sensors, and optical transmission.

Dr. Payne is an Associate Editor or the JOURNAL OF LIGHTWAVE TECHNOLOGY.

*

Robert J. Mears was born in Portsmouth, England, on March 8, 1961. He received the B.A. degree in solid-state and laser physics from Corpus Christi College in 1982, where he had been awarded an Open Scholarship in 1979.

Since 1982, he has been studying for the Ph.D. degree in the Electronics and Information Engineering Department at Southampton University. His research activities comprise passive and active optical-fiber devices, including the development of optical-fiber lasers and amplifiers.

Martin E. Fermann was born in Dubrowno, Poland, on May 9, 1960. He received the M.Sc. degree from the University of Reading, England, in 1984.

In October 1984, he joined the Optical Fiber Group at Southampton University as a Research Assistant where he is working on fiber measurements.

*

Richard I. Laming, photograph and biography not available at time of publication.